

M. TSUBAKI<sup>1</sup>, T. TAKEDA<sup>1</sup>, T. MASTUDA<sup>1</sup>, A. KIMURA<sup>1</sup>, M. YANAE<sup>1,2</sup>, A. MAEDA<sup>1</sup>,  
T. HOSHIDA<sup>1,3</sup>, K. TANABE<sup>3</sup>, S. NISHIDA<sup>1</sup>

## COMBINATION TREATMENT WITH STATINS AND BEZAFIBRATE INDUCES MYOTOXICITY *VIA* INHIBITION OF GERANYLGERANYL PYROPHOSPHATE BIOSYNTHESIS AND RHO ACTIVATION IN L6 MYOBLASTS AND MYOTUBE CELLS

<sup>1</sup>Division of Pharmacotherapy, Kindai University School of Pharmacy, Kowakae, Higashi-Osaka, Japan; <sup>2</sup>Department of Pharmacy, Kindai University Hospital, Ohno-higashi, Osaka-Sayama, Osaka, Japan; <sup>3</sup>Department of Pharmacy, Japanese Red Cross Society Wakayama Medical Center, Wakayama, Japan

Statins and fibrates are frequently used to treat hyperlipidemia; however, these drugs may have adverse effects such as rhabdomyolysis. The incidence of rhabdomyolysis due to fibrates and statins is low (0.0028–0.0096%) when administered as monotherapy, however it increases to 0.015–0.021% when the drugs are used in combination. The mechanism underlying myotoxicity induced by the combination of statins and fibrates is yet unclear. Here, we investigated the mechanisms underlying induced myotoxicity in rat myoblasts L6 and differentiated L6 cells (myotubes) using a combination of statins and fibrates. We found that cell death induced by a combination of fluvastatin or simvastatin with bezafibrate or fenofibrate in L6 myoblasts and myotubes was mediated by inhibition of geranylgeranyl pyrophosphate (GGPP) production. Additionally, the drug combination inhibited Rho activation in L6 myoblasts and myotube cells. In L6 myoblasts, the combination of statins and bezafibrate enhanced p27 expression and induced G1 arrest and apoptosis. Furthermore, combined treatment suppressed Akt activation and enhanced Bim expression in L6 myotubes but did not affect extracellular regulated protein kinase 1/2 activation. These results suggested that combined administration of statins and fibrates induced death of L6 myoblasts and myotube cells by inhibiting GGPP biosynthesis and Rho pathway activation. Supplementation with GGPP may be therapeutically beneficial for preventing myotoxicity associated with combined statin and fibrates treatment.

**Key words:** *statins, fibrate, rhabdomyolysis, myotoxicity, Rho pathway, mevalonate pathway, myoblasts, myotubes, geranylgeranyl pyrophosphate*

### INTRODUCTION

Hyperlipidemia is a risk factor for coronary artery and cerebrovascular disease. Typically, hyperlipidemia is treated using fibrates, which are peroxisome proliferator-activated receptor alpha (PPAR $\alpha$ ) agonists, and statins, which inhibit 3-hydroxy-3-methylglutaryl-coenzyme A (HMG-CoA) reductase. These drugs cause rhabdomyolysis as an adverse effect, albeit at a low rate of occurrence. Rhabdomyolysis is a disorder during which skeletal muscles experience necrosis or damage, and myoglobin and creatine phosphokinase proteins are rapidly released from the muscle into the bloodstream. Myoglobin is filtered by the renal glomeruli and is excreted through urine, however, excessive leakage due to muscle tissue lysis exerts considerable strain on glomeruli and can rapidly lead to renal damage and failure. The consequences of acute kidney failure can be severe, and mortality rate is high (1, 2). When fibrate or statin is administered as monotherapy, the rate of rhabdomyolysis is low (0.0028–0.0096%); however, the incidence increases to 0.015–0.021% when the drugs are used in combination (3). The underlying mechanisms are thus far

unknown, and elucidating these may help administer treatment more rapidly to facilitate early recovery.

Statins inhibit biosynthesis of mevalonate (MVA) by specifically suppressing HMG-CoA reductase in the mevalonic acid pathway, which then inhibits cholesterol formation. Statins also inhibit biosynthesis of isopentenyladenine, geranylgeranyl pyrophosphate (GGPP), farnesyl pyrophosphate (FPP), ubiquinone, squalene, and dolichol in the mevalonic acid pathway. Downstream factors in the mevalonate pathway may be involved in the mechanism of statin-induced myopathy (4). Inhibition of MVA production decreases the concentration of ubiquinone, which is involved in mitochondrial energy transfer, and induces cell death (5). Statins induce apoptosis in various tumor cells by suppressing biosynthesis of GGPP and FPP, which are necessary for prenylation of small GTPases (6). In addition, direct effects of statins on muscle cell membranes have been reported, such as destabilization of membranes due to decreased cholesterol content and decreased chloride permeability of cell membranes (4, 7). Even though various studies examined the pathogenesis of myopathy and the induction of cell death by statins, the underlying mechanisms remain unclear.

Fibrate decreases the function of the mitochondrial respiratory chain by directly binding to PPAR $\alpha$ , a nuclear receptor, thereby decreasing triglyceride levels and lowering lipid levels (8). Depending on the tissue, three subtypes of PPARs occur ( $\alpha$ ,  $\beta$ , and  $\gamma$ ), which strongly affect cell proliferation and differentiation (8). Bezafibrate induces apoptosis in human rhabdomyosarcoma cells by inactivating the Akt pathway (9). However, details of myopathy induction by fibrates are thus far unclear.

Statins increase the transcriptional activity of PPAR $\alpha$ /retinoid X receptor alpha (RXR $\alpha$ ) in hepatoma cells and in mice (10, 11), and bezafibrate suppresses HMG-CoA reductase activity in rat liver microsomes (12). Moreover, fibrates can induce cell death in human fetal rhabdomyosarcoma cells, which is enhanced by concomitant administration of simvastatin (13); the underlying mechanisms are thus far unclear. Fibrate decreases the hepatic metabolic capacity of statins by inhibiting CYP450 metabolic enzymes and increases myotoxicity by increasing blood concentrations of statins (14). However, details of the induction mechanisms of myopathy due to co-administration with statins and fibrates are unknown. In the present study, we examined the mechanism by which combined treatment with statins and bezafibrate-induced cell death in L6 myoblasts and differentiated L6 (myotubes) cells.

## MATERIALS AND METHODS

### Materials

Fluvastatin sodium salt (here referred to as fluvastatin), simvastatin (in lactone form), and bezafibrate and fenofibrate were purchased from FUJIFILM Wako (Tokyo, Japan). These compounds were dissolved in dimethyl sulfoxide (DMSO) and were diluted using phosphate-buffered saline (PBS; 0.05 M, pH 7.4). The compounds were used at DMSO concentrations <0.1% in the assay described below; 0.1% DMSO was used as a control. Water-soluble cholesterol, dolichol, FPP, GGPP, isopentenyl pyrophosphate (IPP), MVA, and ubiquinone were purchased from Sigma-Aldrich (St. Louis, MO, USA), and these compounds were dissolved in dry ethanol and were diluted using PBS (0.05 M, pH 7.4). These reagents were used at dry ethanol concentrations <0.1% in the following assay.

### Cell culture

L6 rat myoblast cells obtained from DS Pharma Biomedical (Osaka, Japan) were cultured in Dulbecco's modified Eagle's medium (DMEM; Sigma-Aldrich, St. Louis, MO, USA) supplemented with 10% fetal bovine serum (FBS; Gibco, Carlsbad, CA, USA), 100  $\mu$ g/mL penicillin (Gibco, Carlsbad, CA, USA), 100 U/mL streptomycin (Gibco, Carlsbad, CA, USA), and 25 mM 4-(2-hydroxyethyl)-1-piperazineethanesulfonic acid (FUJIFILM Wako, Osaka, Japan) in an atmosphere containing 5% CO<sub>2</sub>.

L6 cells were cultured in DMEM supplemented with 10% FBS after reaching 80% confluence and were then transferred to DMEM supplemented with 2% horse serum (differentiation medium) for 10 days to induce myotube formation. L6 myoblasts were passaged 4–8 times.

### Cell viability

Cell viability was analyzed by tetrazolium dye production using a WST-8 assay kit (Seikagaku, Tokyo, Japan), as previously described (15). Briefly, L6 myoblasts ( $2 \times 10^4$  cells/mL) were plated in 96-well plates and were incubated with fluvastatin (0.25–

1.0  $\mu$ M), simvastatin (1–5  $\mu$ M), bezafibrate (50–200  $\mu$ M), or fenofibrate (50–200  $\mu$ M) for one, two, or three days. L6 myotubes were treated with (0.05–0.5  $\mu$ M), simvastatin (0.5–5  $\mu$ M), bezafibrate (100–400  $\mu$ M), or fenofibrate (100–400  $\mu$ M) for three, five, or seven days. Absorbance of each well was measured at 492 nm using a microplate reader (SK601; Seikagaku, Tokyo, Japan).

### Western blotting

L6 myoblasts and L6 myotubes cultured under various conditions were lysed with a lysis buffer (20 mM Tris-HCl, pH 8.0, Sigma-Aldrich, St. Louis, MO, USA), 150 mM NaCl (FUJIFILM Wako, Osaka, Japan), 2 mM ethylenediaminetetraacetic acid (FUJIFILM Wako, Osaka, Japan), 100 mM NaF (Sigma-Aldrich, St. Louis, MO, USA), 1% NP-40 (FUJIFILM Wako, Osaka, Japan), 1  $\mu$ g/mL leupeptin (Sigma-Aldrich, St. Louis, MO, USA), 1  $\mu$ g/mL pepstatin A (Sigma-Aldrich, St. Louis, MO, USA), and 1 mM phenylmethyl sulfonyl fluoride (PMSF, Sigma-Aldrich, St. Louis, MO, USA). A protein aliquot (20  $\mu$ g) of each extract was resolved using 10% sodium dodecyl sulfate-polyacrylamide gel electrophoresis (SDS-PAGE) and was transferred to a polyvinylidene fluoride membrane (GE Healthcare, Buckinghamshire, UK). The membranes were blocked with a solution containing 3% skim milk, followed by overnight incubation at 4°C with each of the following antibodies: anti-phospho-c-Jun N-terminal kinase (JNK) (#9251), anti-phospho-p38 mitogen-activated protein kinase (MAPK) (#9211), anti-phospho-Akt (#9272), anti-phospho-extracellular signal-regulated kinase (ERK)1/2 (#9101), anti-JNK (#9252), anti-p38MAPK (#9211), anti-Akt (#9272), and anti-ERK1/2 (#9102) antibodies (all procured from Cell Signaling Technology, Beverly, MA, USA), anti-p27 (F-8), anti-p21 (F-5), anti-p53 (DO-1), anti-myogenin (F5D), and anti-myoblast determination protein 1 (Myo D; M-318) antibodies (all procured from Santa Cruz Biotechnology, Santa Cruz, CA, USA), and anti-myosin heavy chain (MHC; clone A4.1025) and anti- $\beta$ -actin (AC-74), procured from Sigma-Aldrich. Subsequently, the membranes were incubated for 1 h at room temperature with anti-rabbit sheep IgG antibody coupled with horseradish peroxidase or anti-mouse horse IgG antibody coupled with horseradish peroxidase (Cell Signaling Technology, Beverly, MA, USA). Reactive proteins were visualized using Luminata Forte (Merck Millipore, Beverly, MA, USA) according to the manufacturer's instructions. The levels of phosphorylated proteins, cell cycle-related proteins, and myogenic marker proteins were determined after normalization to the total proteins or  $\beta$ -actin present in the cell lysates.

### Rho pull-down assay

Rho activation was analyzed using a Rhotekin pull-down assay kit (Thermo Fisher Scientific, Waltham, MA, USA) as previously described (16). Briefly, cells were lysed in 500  $\mu$ L lysis buffer containing 50 mM Tris (pH 7.4), 10 mM MgCl<sub>2</sub>, 500 mM NaCl, 1% Triton X-100, 0.1% SDS, 0.5% sodium deoxycholate, 10  $\mu$ g/mL of each aprotinin and leupeptin, and 1 mM PMSF. Lysates were cleared by centrifugation at 12,000 $\times$ g and 4°C for 10 min, and 500  $\mu$ g of each lysate was then incubated with 45  $\mu$ g GST fusion protein containing the Rho-binding domain of Rhotekin bound to glutathione-Sepharose beads (Thermo Fisher Sci., Waltham, MA, USA) for 1 h. After binding, the samples were washed three times using lysis buffer. Bound proteins were fractionated on 10% SDS-PAGE gels and were immunoblotted using a monoclonal antibody against Rho (Thermo Fisher Sci., Waltham, MA, USA). Total cell lysates were also blotted with Rho antibody as a loading control. The level of active Rho was determined after normalization to the total amount of Rho present in the cell lysates.

### Cell cycle analysis

The cell cycle was analyzed using propidium iodide (PI; Sigma-Aldrich, St. Louis, MO, USA) as previously described (17). Briefly, cells were washed twice with PBS and were resuspended in 70% ethanol; after 24 h, the cells were washed twice with PBS and were then resuspended in DNAase-free RNAase A (Sigma-Aldrich, St. Louis, MO, USA) and PI. After incubation at room temperature for 15 min, cells were analyzed using a BD LSRFortessa flow cytometer (Becton Dickinson, Bedford, MA, USA).

### Caspase-3 activity analysis

The activity of caspase-3 was determined using a caspase-3/CPP32 fluorometric assay kit (BioVision, Mountain View, CA, USA) according to the manufacturer's instructions. Myoblasts or myotubes were treated with fluvastatin, simvastatin, or bezafibrate alone or in combination for two or five days. After incubation, the cells were washed with PBS and were lysed using lysis buffer included in the caspase-3/CPP32 fluorometric assay kit. The cell lysates were treated with 1 mM Asp-Glu-Val-Asp-7-amino-4-trifluoromethylcoumarin (AFC) at 37°C for 1 h. Concentrations of AFC released from the substrate were measured using a fluorescence spectrophotometer (Hitachi, Tokyo, Japan) at emission and excitation wavelengths of 505 and 400 nm, respectively.

### Quantitative real-time polymerase chain reaction (PCR)

Total RNA was isolated using RNAiso (Takara Biomedical, Shiga, Japan), and cDNA was synthesized from purified total RNA using a PrimeScript First-Strand Synthesis System (Takara Biomedical, Shiga, Japan). The cDNA was subjected to quantitative real-time PCR in a 96-well plate using SYBR Premix Ex Taq (Takara Biomedical, Shiga, Japan) and a Thermal Cycler Dice Real Time System (Takara Biomedical, Ohtsu, Japan), analyses were conducted according to the manufacturer's instructions. The PCR conditions for glyceraldehyde-3-phosphate dehydrogenase (GAPDH), myogenin, MyoD, and myosin heavy chain (MHC) gene sequence amplification were 94°C for 2 min, followed by 40 cycles of 94°C for 0.5 min, 50°C for 0.5 min, and 72°C for 0.5 min.

The following primer sequences were used:

myogenin: 5'-AGT GCC ATC CAG TAC ATT GAG CG-3' (5'-primer) and 5'-GGG TGG AAT TAG AGG CGC ATT A-3' (3'-primer),  
MyoD: 5'-CAC ACT TCC CCA CTA CGG TGC-3' (5'-primer) and 5'-CAC TGT AGT AGG CGG CGT CGT AG-3' (3'-primer),  
MHC: 5'-AGA AGG CCA AGA AAG CCA T-3' (5'-primer) and 5'-TTT TTT ATC TCC CAA AGT CG-3' (3'-primer), and  
GAPDH: 5'-CTC TGG AAA GCT GTG GCG TGA T-3' (5'-primer) and 5'-CTG GGA TGG AAT TGT GAG GGG G-3' (3'-primer). GAPDH was used as an internal control to normalize the measurements for each sample. Cycle threshold (Ct) values were established, and relative differences in expression with respect to control cells were determined using the  $2^{-\Delta\Delta Ct}$  method.

### Statistical analysis

All results are shown as means  $\pm$  standard deviation of several independent experiments. All analyses were performed using one-way analysis of variance with Dunnett's test. Statistical significance is reported at  $P < 0.05$ . Drug interactions were analyzed using a combination index (CI) as previously described (18); a CI < 1.0 indicated synergy, whereas a CI > 1 indicated antagonism.

## RESULTS

### *Effect of fluvastatin, simvastatin, bezafibrate, and fenofibrate alone and in combination with fluvastatin or simvastatin and bezafibrate or fenofibrate on L6 myoblast cell viability*

Our previous studies have shown that fluvastatin is 2.5- to 5-fold more effective than simvastatin (19, 20). Therefore, the dosage of simvastatin was 2.5- to 5-fold higher than that of fluvastatin. L6 cells were treated with fluvastatin (0.25–1.0  $\mu$ M), simvastatin (1–5  $\mu$ M), bezafibrate (50–200  $\mu$ M), or fenofibrate (50–200  $\mu$ M) and cell survival was assessed and compared with that of control cells. Fluvastatin, simvastatin, bezafibrate, and fenofibrate induced cell death in a concentration- and time-dependent manner (Fig. 1A). The combination of fluvastatin (0.5  $\mu$ M) or simvastatin (1  $\mu$ M) with bezafibrate (100  $\mu$ M) or fenofibrate (100  $\mu$ M), concentrations that reduced survival rates by approximately 80%, significantly induced cell death, and CI values also showed a synergistic effect (Fig. 1B). Based on these results, we used 100  $\mu$ M bezafibrate or 100  $\mu$ M fenofibrate with 0.5  $\mu$ M fluvastatin or 1  $\mu$ M simvastatin, which was cytotoxic to L6 cells.

### *Inhibitory effects of mevalonate pathway metabolites on combined treatment with statins and fibrates induced cell death*

We examined the inhibitory effects of cholesterol, dolichol, FPP, GGPP, IPP, MVA, and ubiquinone, which are biosynthesized in the mevalonate pathway, on cell death induced by administration with bezafibrate or fenofibrate alone, and combined treatment with statins and bezafibrate. L6 cells were pretreated with cholesterol, dolichol, FPP, GGPP, IPP, MVA, and ubiquinone for 4 h and were then administrated with 100  $\mu$ M bezafibrate or 100  $\mu$ M fenofibrate alone, and co-treated with 0.5  $\mu$ M fluvastatin or 1  $\mu$ M simvastatin and 100  $\mu$ M bezafibrate or 100  $\mu$ M fenofibrate. The number of viable cells was recorded after three days. Induction of cell death was confirmed in the presence of cholesterol, dolichol, FPP, IPP, and ubiquinone, but cell death was significantly suppressed by co-treatment with MVA and GGPP (Fig. 1C). In addition, pretreatment with cholesterol, dolichol, FPP, GGPP, IPP, MVA, or ubiquinone did not affect bezafibrate and fenofibrate induced cell death (Fig. 1C).

### *Effect of combined treatment with statins and bezafibrate on Ras downstream signaling molecules*

GGPPs are involved in prenylation of small GTPases such as Ras and Rho and activate downstream signaling factors by anchoring them to the membrane. As cell death induced by the co-treatment of statins and bezafibrate was suppressed by pretreatment with GGPP, we investigated the activation of the main downstream signaling factors p38MAPK, Akt, and ERK1/2. Treatment with fluvastatin, simvastatin, or bezafibrate alone and combined treatment with statins and bezafibrate did not affect activation of p38MAPK, Akt, and ERK1/2 in L6 cells (Fig. 2A and 2B). These results indicated that Ras signaling pathways, such as p38MAPK, Akt, and ERK1/2, are not involved in L6 myoblast cell death induced by co-treatment with statins and bezafibrate.

### *Combined treatment with statins and bezafibrate suppresses Rho activation*

As the Ras pathway was not involved in the induction of cell death by the combined administration of statins and bezafibrate, we examined the involvement of Rho in GGPP.

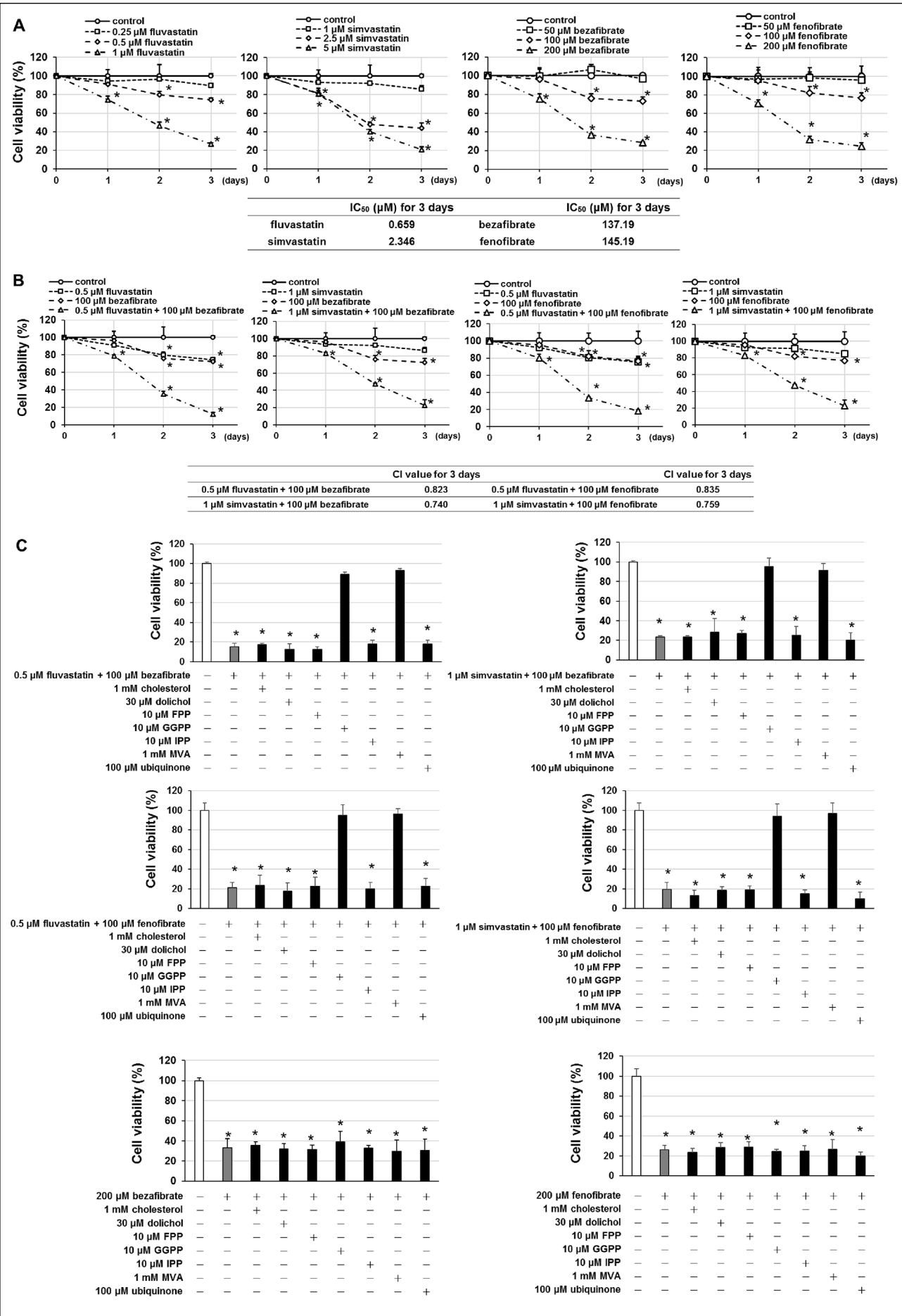


**Fig. 1.** Effects of fluvastatin, simvastatin, bezafibrate, and fenofibrate on rat L6 myoblast cell viability. Cell viability after treatment with (A): fluvastatin, simvastatin, bezafibrate, and fenofibrate alone or (B): combination treatment with statins and fibrates in L6 myoblast cells as determined using a WST-8 assay. Cells were treated with various concentrations of fluvastatin, simvastatin, bezafibrate, and fenofibrate alone, or in combination with 0.5  $\mu$ M fluvastatin or 1  $\mu$ M simvastatin and 100  $\mu$ M bezafibrate or 100  $\mu$ M fenofibrate for one, two, or three days. Shown are the means  $\pm$  standard deviation (SD) of five independent replicates. The IC<sub>50</sub> and CI values of fluvastatin, simvastatin, bezafibrate, fenofibrate, or of these drugs in combination in L6 cells were noted; \* $P$ <0.01 vs. controls (ANOVA with Dunnett's test). (C): L6 cells were pretreated for 4 h with 1 mM cholesterol, 30  $\mu$ M dolichol, 10  $\mu$ M farnesyl pyrophosphate (FPP), 10  $\mu$ M geranylgeranyl pyrophosphate (GGPP), 10  $\mu$ M isopentenyl pyrophosphate (IPP), 1 mM mevalonate (MVA), or 100  $\mu$ M ubiquinone, followed by treatment with bezafibrate alone and a combination of fluvastatin or simvastatin and bezafibrate or fenofibrate for 72 h. Shown are the means  $\pm$ SD of five independent replicates. \* $P$ <0.01 vs. controls (ANOVA with Dunnett's test).

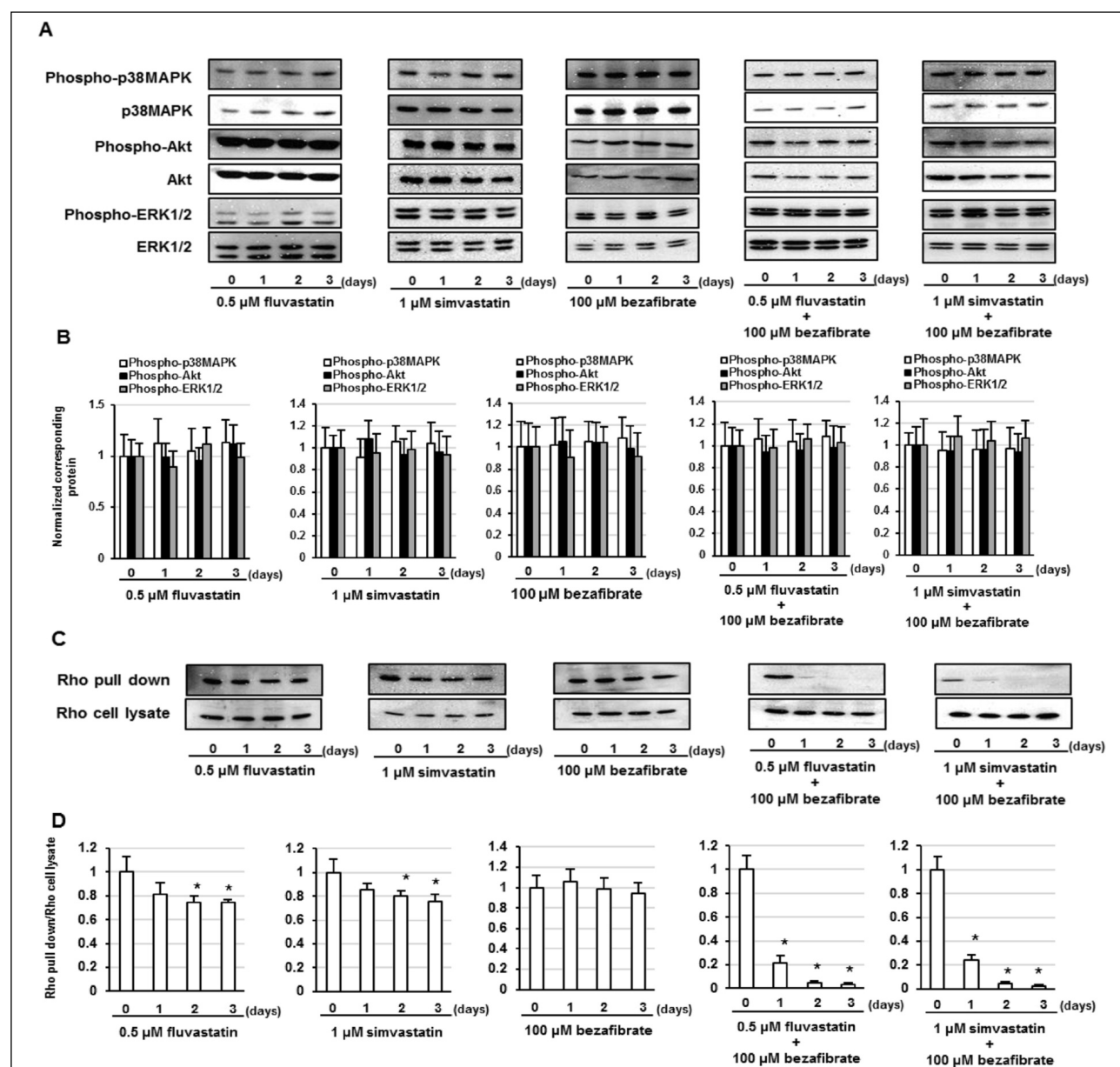


**Fig. 2.** Combined treatment with statins and bezafibrate suppresses the activation of the Rho in L6 cells. (A): L6 cells were administrated with 0.5  $\mu$ M fluvastatin or 1  $\mu$ M simvastatin and 100  $\mu$ M bezafibrate alone or in combination for 1, 2, or 3 days. The cell lysates were subjected to Western blotting using phosphorylated p38MAPK (phospho-p38MAPK), phosphorylated Akt (phospho-Akt), phosphorylated ERK1/2 (phospho-ERK1/2), p38MAPK, Akt, and ERK1/2 antibodies. (B): Amounts of phospho-p38MAPK, phospho-Akt, or phospho-ERK1/2 were measured and standardized to the amounts of the p38MAPK, Akt, or ERK1/2. Shown are the means  $\pm$  SD of three independent replicates. \* $P$ <0.01 vs. controls (ANOVA with Dunnett's test). (C): L6 cells were administrated with concentrations of 0.5  $\mu$ M fluvastatin, 1  $\mu$ M simvastatin, and 100  $\mu$ M bezafibrate alone, or in combination for 1, 2, or 3 days. L6 cells were lysed in lysis buffer and incubated with equal volumes of lysates in agarose beads conjugated with Rhotekin. Rhotekin-conjugated Rho proteins were detected by Western blotting using antibody of Rho-A, -B, and -C. (D): Amounts of Rho pull-down were measured and standardized to the amounts of the total Rho. Shown are the means  $\pm$  SD of three independent replicates. \* $P$ <0.01 vs. controls (ANOVA with Dunnett's test).

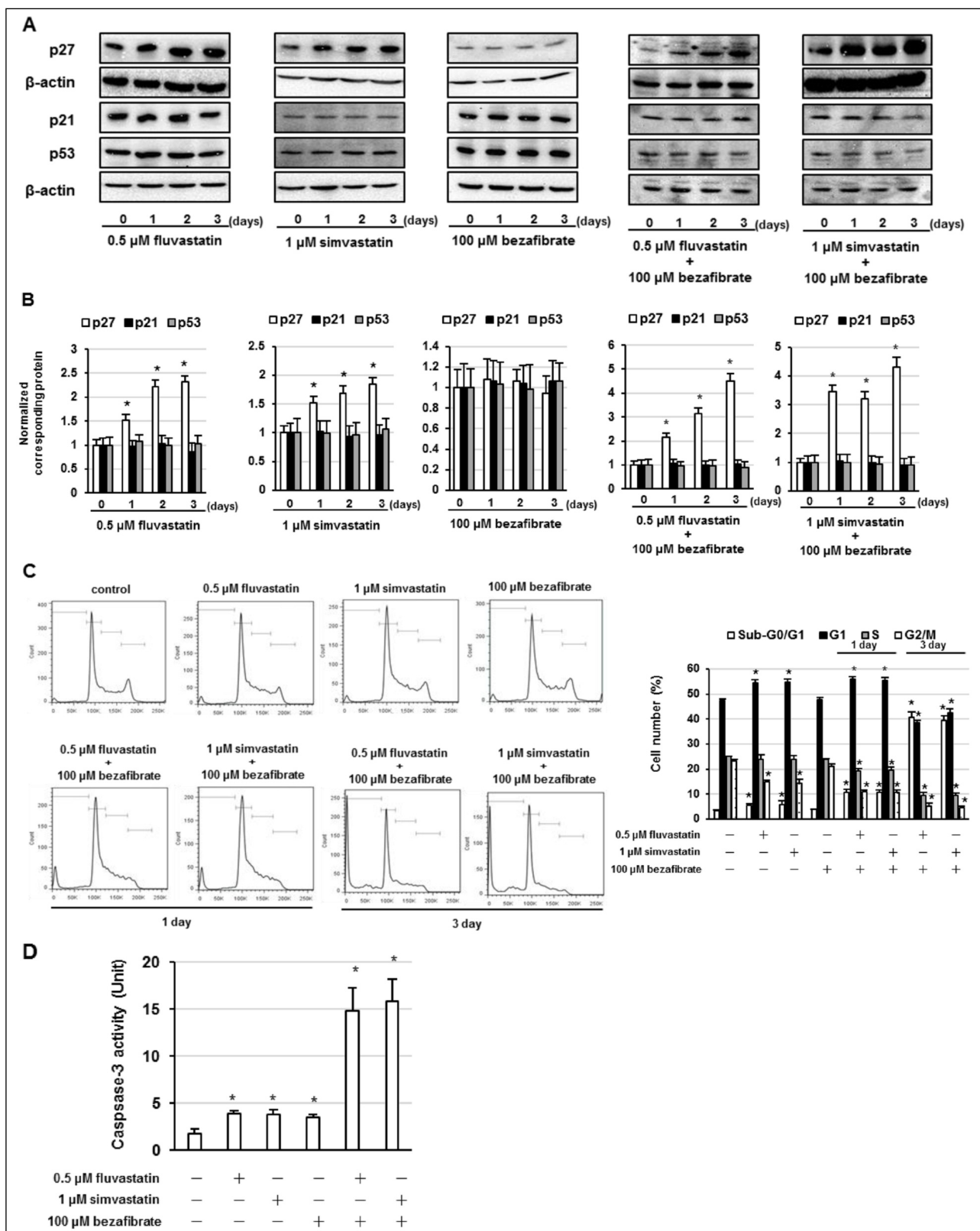


**Fig. 3.** Combined treatment with statins and bezafibrate enhances p27 expression and G1 arrest in L6 cells. (A): L6 cells were administrated with 0.5  $\mu$ M fluvastatin or 1  $\mu$ M simvastatin and 100  $\mu$ M bezafibrate alone or in combination for one, two, or three days. The cell lysates were subjected to Western blotting using p27, p21, p53, and  $\beta$ -actin antibodies. (B): Amounts of p27, p21, or p53 were measured and standardized to the amounts of the  $\beta$ -actin; upper  $\beta$ -actin was used for standardization of p27, and lower  $\beta$ -actin was used for standardization of p21 or p53. Shown are the means  $\pm$  SD of three independent replicates. \* $P$  < 0.01 vs. controls (ANOVA with Dunnett's test). (C): Changes in cell cycle distribution were examined by flow cytometry. The relative proportion of cells in each phase of the cell cycle was shown. Shown are the means  $\pm$  SD of five independent replicates. \* $P$  < 0.01 vs. controls (ANOVA with Dunnett's test). (D): Caspase-3 activities are showed in picomoles/h/mg protein as the quantity of the caspase-3 substrate DEVD-AFC cleaved by proteolysis. Shown are the means  $\pm$  SD of five independent replicates. \* $P$  < 0.01 vs. controls (ANOVA with Dunnett's test).

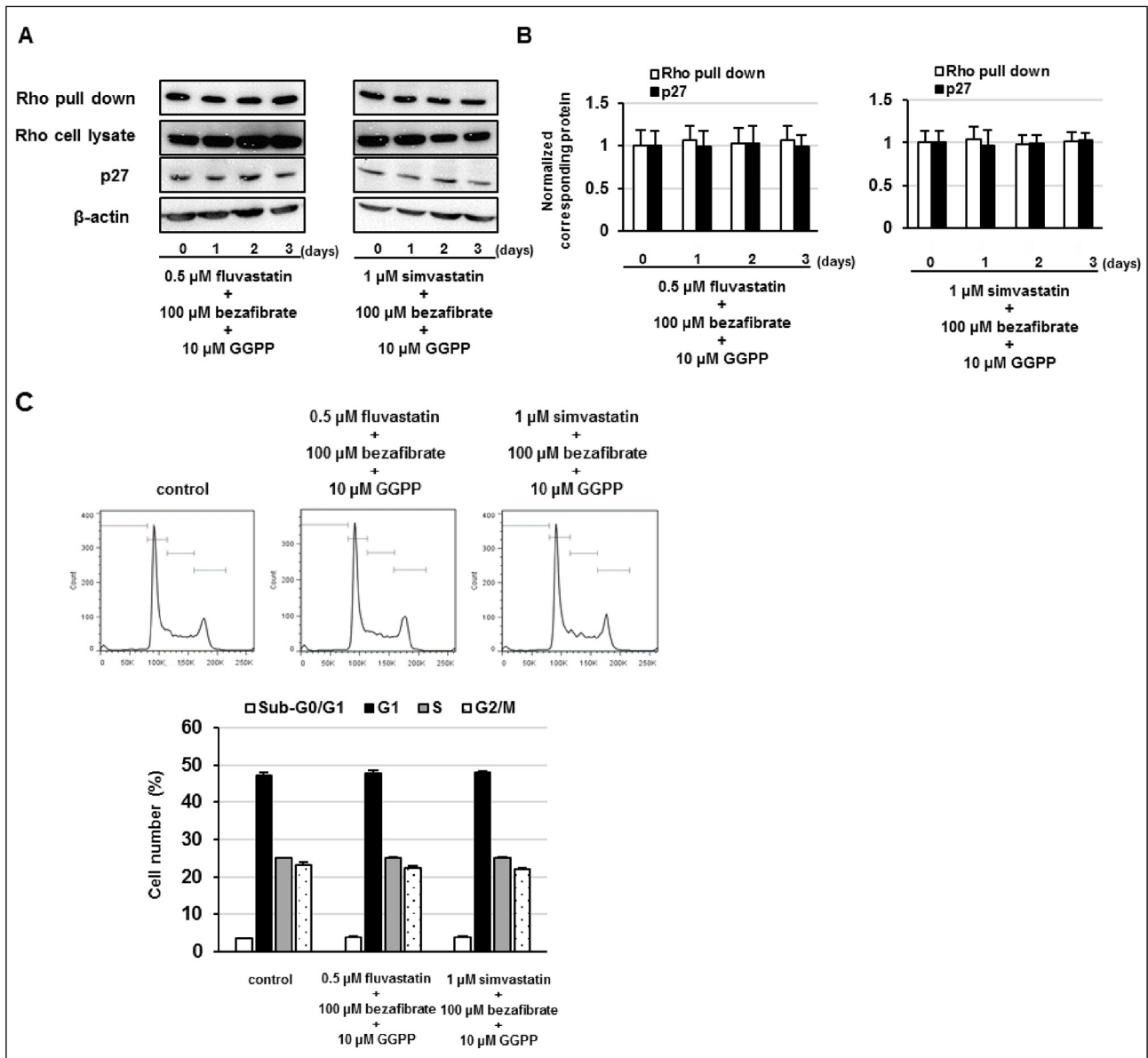


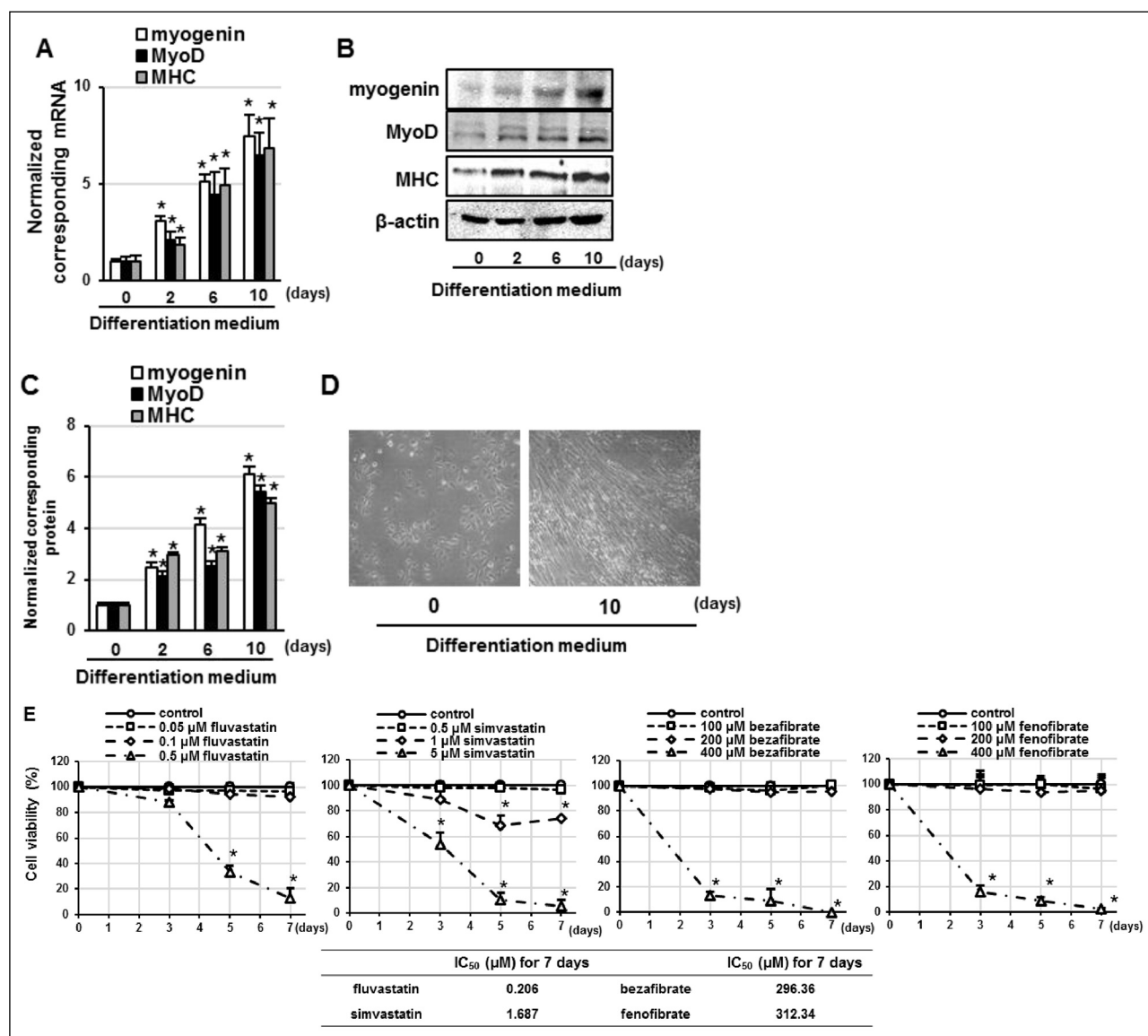
**Fig. 4.** Pretreatment with GGPP inhibited the co-treatment with statins and bezafibrate induced Rho inactivation, p27 expression, and cell cycle arrest. L6 cells were pretreated with 10  $\mu$ M geranylgeranyl pyrophosphate (GGPP) for 4 h and were then co-treated with fluvastatin or simvastatin and bezafibrate for one, two, or three days. (A): Images of Western blots for the Rho-GTP form (Rho pull-down), Rho cell lysate, p27, and  $\beta$ -actin. (B): Amounts of Rho pull-down or p27 were measured and standardized to the amounts of the Rho cell lysate or  $\beta$ -actin. Shown are the means  $\pm$  SD of three independent replicates. \* $P$ <0.01 vs. controls (ANOVA with Dunnett's test). (C): Changes in cell cycle distribution were examined by flow cytometry. The relative proportion of cells in each phase of the cell cycle was shown. Shown are the means  $\pm$  SD of five independent replicates. \* $P$ <0.01 vs. controls (ANOVA with Dunnett's test).

Although treatment with fluvastatin and simvastatin alone weakly suppressed Rho activation, bezafibrate alone did not affect Rho activation, and combined treatment with statins and bezafibrate significantly suppressed Rho activation in L6 cells (Fig. 2C and 2D). Activation of Rho promotes cell cycle progression by suppressing cell cycle-dependent kinase inhibitors such as p27, p21, and p53 (21). We thus examined the effect of treatment with statins and bezafibrate alone and in combination on p27, p21, and p53 expression and cell cycle progression in L6 cells. Fluvastatin and simvastatin weakly enhanced p27 expression and increased the cell population at the sub-G0/G1 and G1 phases for three days, but did not affect p21 and p53 expression (Fig. 3A-3C). Bezafibrate alone did not affect p27, p21, or p53 expression, or cell cycle progression

(Fig. 3A-3C). Combined administration of statins and bezafibrate strongly enhanced p27 expression and increased the cell population at the sub-G0/G1 and G1 phases for one and three days, but did not affect p21 and p53 expression (Fig. 3A-3C). In addition, combined treatment with statins and bezafibrate significantly increased caspase-3 activity, whereas statin and bezafibrate administration alone only weakly enhanced caspase-3 activity (Fig. 3D). Moreover, pretreatment with GGPP suppressed the combination of statins and bezafibrate-induced p27 expression and G1 arrest and restored Rho activation in L6 cells (Fig. 4). These results suggested that combination of statins with bezafibrate induced myoblast cell death by suppressing GGPP synthesis and Rho activation and enhanced p27 expression and G1 arrest.

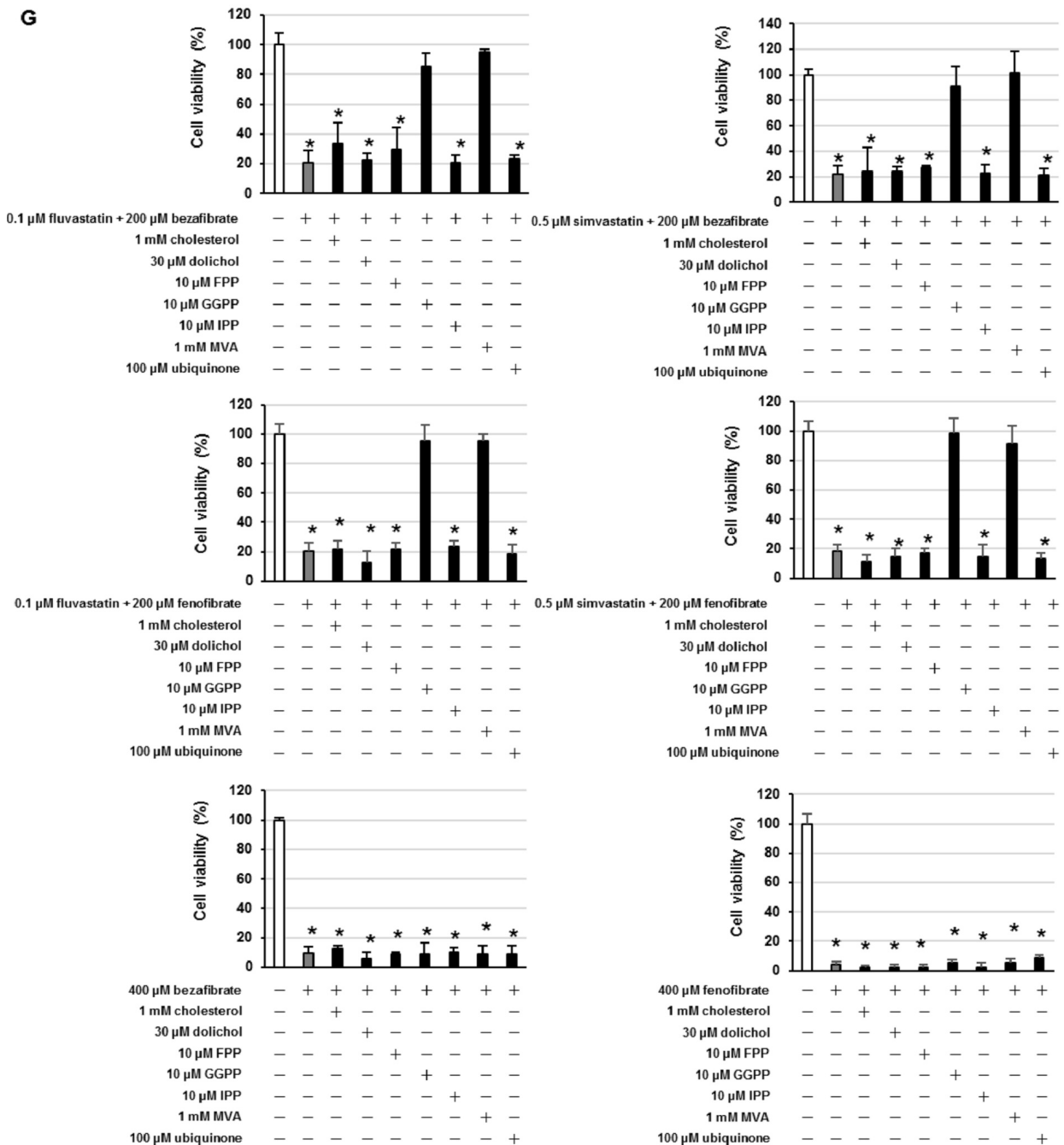
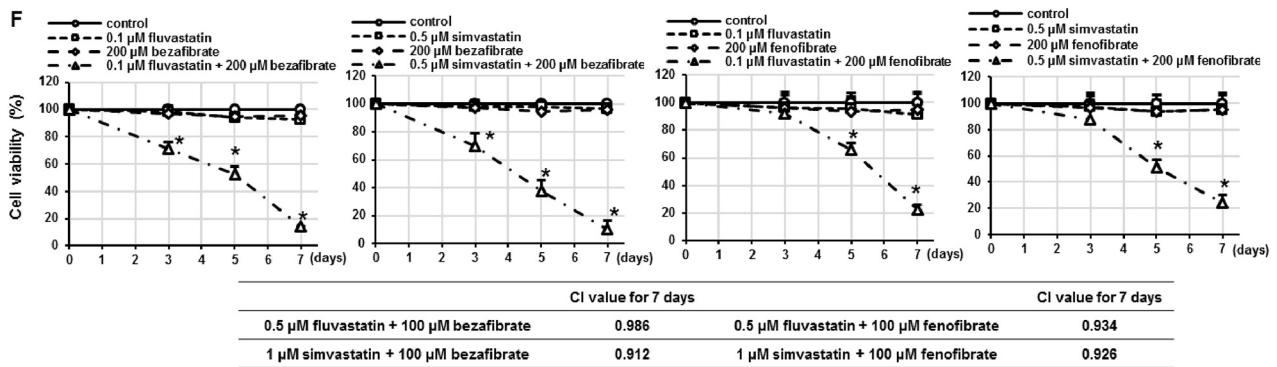
Effect of treatment with fluvastatin, simvastatin, bezafibrate, and fenofibrate alone, and treatment with fluvastatin or simvastatin combined with bezafibrate or fenofibrate on L6 myotube cell viability

The combination of statins and bezafibrate induced cell death by suppressing Rho activation and promoting G1 arrest. Next, we investigated whether combined treatment with statins and fibrates would induce cell death in L6



**Fig. 5.** Effects of fluvastatin, simvastatin, bezafibrate, and fenofibrate on L6 myotube cell viability. (A-D): Confirmation of L6 differentiation. L6 cells were cultured with DMEM containing 10% FBS after growth to 80% confluence, and then were transferred to DMEM containing 2% horse serum (differentiation medium) for 10 days to induce myotube formation. (A): Using the extracted total RNA, myogenin, MyoD, or MHC mRNA expression was analyzed by real-time polymerase chain reaction (PCR). The results are corrected for glyceraldehyde 3-phosphate dehydrogenase (GAPDH) mRNA and then calculated as a control ratio. Shown are the means  $\pm$  SD of five independent replicates.  $*P < 0.01$  vs. controls (ANOVA with Dunnett's test). (B): Images of Western blots for the myogenin, MyoD, MHC, and  $\beta$ -actin. (C): Amounts of myogenin, MyoD, or MHC were measured and standardized to the amounts of  $\beta$ -actin. Shown are the means  $\pm$  SD of three independent replicates.  $*P < 0.01$  vs. controls (ANOVA with Dunnett's test). (D): Myotubes were fixed in absolute methanol for 10 min and were observed using light microscopy. (E, F): Cell viability after treatment with (E): fluvastatin, simvastatin, bezafibrate, and fenofibrate alone or (F): combination treatment with statins and fibrates in L6 myotube cells, as determined using a WST-8 assay. The cells were treated with diverse concentrations of fluvastatin, simvastatin, bezafibrate, and fenofibrate alone, or by combination with 0.1  $\mu$ M fluvastatin or 0.5  $\mu$ M simvastatin and 200  $\mu$ M bezafibrate or 200  $\mu$ M fenofibrate for three, five, or seven days. Shown are the means  $\pm$  SD of five independent replicates. The IC<sub>50</sub> and CI values of fluvastatin, simvastatin, bezafibrate, and fenofibrate, or combination of these drugs in L6 myotube cells were noted;  $*P < 0.01$  vs. controls (ANOVA with Dunnett's test). (G): L6 myotube cells were pretreated for 4 h with 1 mM cholesterol, 30  $\mu$ M dolichol, 10  $\mu$ M farnesyl pyrophosphate (FPP), 10  $\mu$ M geranylgeranyl pyrophosphate (GGPP), 10  $\mu$ M isopentenyl pyrophosphate (IPP), 1 mM mevalonate (MVA), or 100  $\mu$ M ubiquinone, followed by treatment with bezafibrate or fenofibrate alone, combination with fluvastatin or simvastatin and bezafibrate or fenofibrate for seven days. Shown are the means  $\pm$  SD of five independent replicates.  $*P < 0.01$  vs. controls (ANOVA with Dunnett's test).





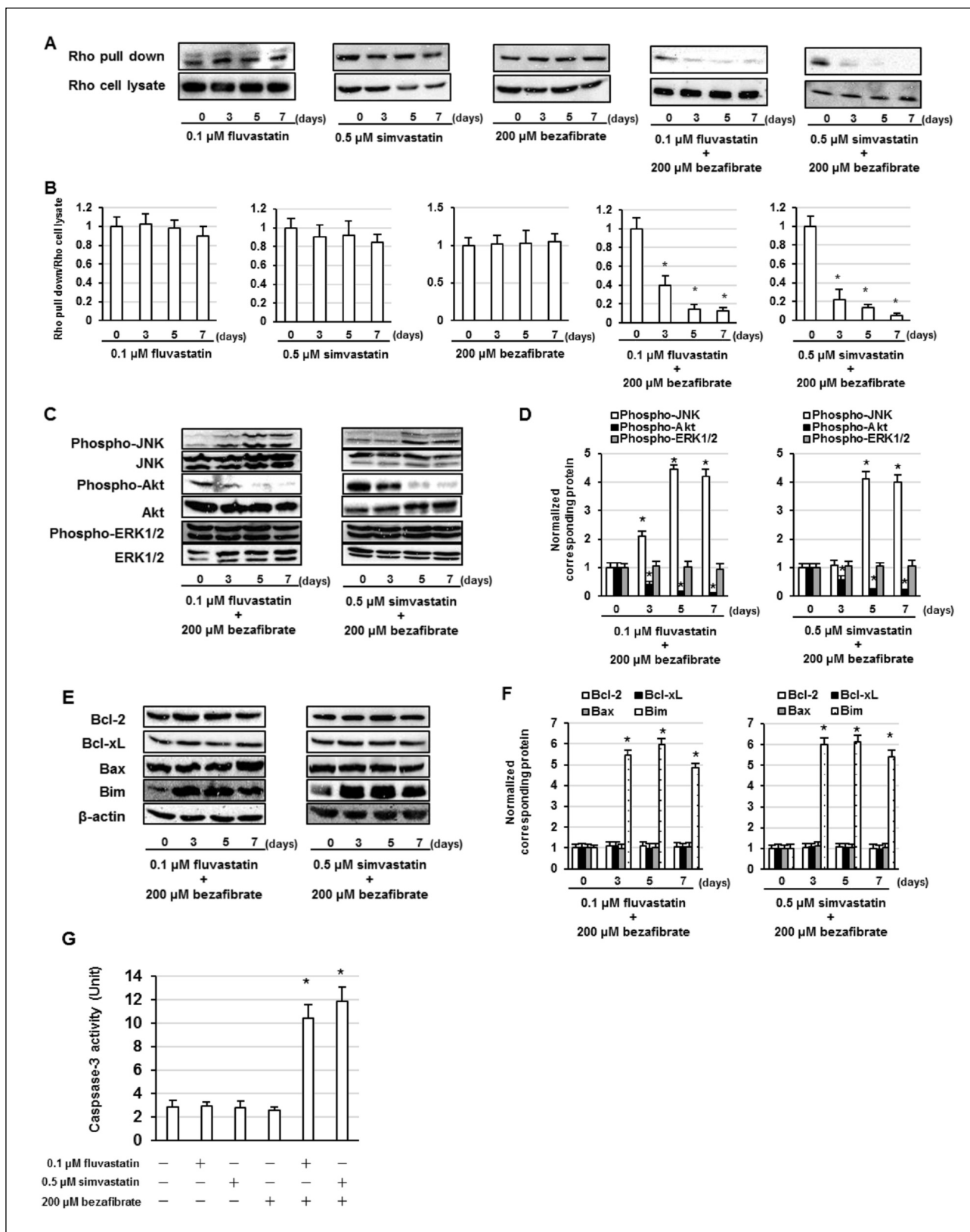


**Fig. 6.** Combined treatment with statins and bezafibrate suppresses activation of the Rho in L6 myotube cells. (A): L6 myotube cells were treated with 0.1  $\mu$ M fluvastatin or 0.5  $\mu$ M simvastatin and 200  $\mu$ M bezafibrate alone or in combination for three, five, or seven days. L6 myotube cells were lysed in lysis buffer and were incubated with equal volumes of lysates in agarose beads conjugated with Rhotekin. Rhotekin-conjugated Rho proteins were detected by western blotting using antibody of Rho-A, -B, and -C. (B): Amounts of Rho pull-down were measured and standardized to the amounts of the total Rho. Shown are the means  $\pm$  SD of three independent replicates. \* $P$ <0.01 vs. controls (ANOVA with Dunnett's test). (C): The cell lysates were subjected to Western blotting using phosphorylated JNK (phospho-JNK), phosphorylated Akt (phospho-Akt), phosphorylated ERK1/2 (phospho-ERK1/2), JNK, Akt, and ERK1/2 antibodies. (D): Amounts of phospho-JNK, phospho-Akt, or phospho-ERK1/2 were measured and standardized to the amounts of the JNK, Akt, or ERK1/2. Shown are

the means  $\pm$  SD of three independent replicates. \* $P$ <0.01 vs. controls (ANOVA with Dunnett's test). (E): The cell lysates were subjected to Western blotting using Bcl-2, Bcl-xL, Bax, Bim, and  $\beta$ -actin antibodies. (F): Amounts of Bcl-2, Bcl-xL, Bax, or Bim were measured and standardized to the amount of  $\beta$ -actin. Shown are the means  $\pm$  SD of three independent replicates. \* $P$ <0.01 vs. controls (ANOVA with Dunnett's test). (G): Caspase-3 activities are showed in picomoles/h/mg protein as the quantity of the caspase-3 substrate DEVD-AFC cleaved by proteolysis. Shown are the means  $\pm$  SD of five independent replicates. \* $P$ <0.01 vs. controls (ANOVA with Dunnett's test).

differentiated myotube cells. First, we examined the differentiation of L6 cells into myotube cells using a differentiation medium (DMEM containing 2% horse serum). Culturing L6 cells with differentiation medium increased the expression of the myogenic markers myogenin, MyoD, and MHC mRNA and protein, and promoted long tube formation for 10 days (Fig. 5A-D). Next, we investigated the cytotoxic effects of fluvastatin, simvastatin, bezafibrate fenofibrate alone, and of combined treatment with fluvastatin, simvastatin, bezafibrate, and fenofibrate on L6 myotube cells. Cells were treated with fluvastatin (0.05–0.5  $\mu$ M), simvastatin (0.5–5  $\mu$ M), bezafibrate (100–400  $\mu$ M), or fenofibrate (100–400  $\mu$ M), and viability was assessed and compared with that of control cells. Although fluvastatin, simvastatin, bezafibrate, and fenofibrate alone significantly induced cell death at concentrations of 0.5, 5, and 400  $\mu$ M, they did not affect cell viability at 0.05, 0.5, and 200  $\mu$ M (Fig. 5E). Based on these results, concentrations of 0.05  $\mu$ M fluvastatin or 0.5  $\mu$ M simvastatin and 200  $\mu$ M bezafibrate or 200  $\mu$ M fenofibrate, which are not cytotoxic to L6 myotube cells, were used to examine the effects of statins and fibrates combination on cell death. The combination of 0.05  $\mu$ M fluvastatin or 0.5  $\mu$ M simvastatin and 200  $\mu$ M bezafibrate or 200  $\mu$ M fenofibrate significantly induced cell death, and CI values also showed a synergistic effect (Fig. 5F).

#### *Inhibitory effect of co-treatment with statins and bezafibrate on Rho activation and downstream signaling molecules*

We investigated the effects of intermediate metabolism of the mevalonate pathway on L6 myotube cell death induced by co-treatment with statins and fibrates. Pretreatment with GGPP or MVA suppressed L6 myotube cell death due to co-administration of statins and fibrates, similar to the induction of cell death in L6 cells by combined administration of statins and fibrates (Fig. 5G). In addition, pretreatment with cholesterol, dolichol, FPP, GGPP, IPP, MVA, or ubiquinone did not affect bezafibrate and fenofibrate induced cell death (Fig. 5G). Moreover, combined treatment with statins and bezafibrate suppressed Rho activation; however, treatment with statins or bezafibrate alone did not affect Rho activation in L6 myotube cells (Fig. 6A and 6B). As G1 arrest had already occurred in differentiated L6 cells, we examined the downstream signaling of Rho, including JNK, Akt, and ERK1/2, in combination with statins and bezafibrate. We found that the statin and bezafibrate combination treatment inhibited Akt activation and enhanced JNK activation in L6 myotube cells (Fig. 6C and 6D). Decreasing Akt activation or increasing JNK activation is regulated by Bcl-2 family proteins, which are apoptosis-regulated factors (15, 22). Co-treatment with statins and bezafibrate enhanced Bim expression but did not affect Bcl-2, Bcl-xL, or Bax expression, leading to the induction of caspase-3 activity (Fig. 6E-6G). In addition, pretreatment with GGPP inhibited the combined treatment with statins and bezafibrate-induced suppression of Rho and Akt activation and enhanced JNK activation and Bim expression in L6 myotube cells (Fig. 7A-7D). Moreover, LY294002, a phosphoinositide 3-kinase inhibitor, induced cell

death in L6 myotube cells by suppressing Akt activation and increasing JNK activation and Bim expression (Fig. 7E-7G). However, at a concentration that inhibited JNK activation, SP600125, a JNK inhibitor, did not suppress cell death due to combined treatment with statins and bezafibrate (Fig. 7H-7I). These results indicated that combined treatment with statins and bezafibrate induced L6 myotube cell death through suppression of GGPP biosynthesis and Rho/Akt pathway activation and enhanced Bim expression.

## DISCUSSION

In this study, we demonstrated that co-administration of statins and fibrates induced cell death through suppression of GGPP biosynthesis in L6 myoblasts and myotube cells, but it did not affect cholesterol, dolichol, FPP, IPP, and ubiquinone biosynthesis. Ubiquinone (referred to as coenzyme Q10) is an essential electron carrier between complexes I or II and complex III in the inner mitochondrial membrane, is important as an antioxidant and promotes ATP production, however, statin-induced myopathy is not involved in suppression of ubiquinone production in rats (4). In addition, a meta-analysis showed that treatment with ubiquinone in statin-induced myopathy patients did not yield considerable overall benefit (23). Moreover, dolichol promotes N-glycosylation of proteins and statin-induced myopathy may be involved in the suppression of dolichol production, leading to impaired receptor expression and structural protein production (5). Cholesterol reduction by statins induces modification of sodium, potassium, and chloride channels, thereby causing myopathy (5); however, pretreatment with cholesterol and dolichol does not reverse statin-induced apoptosis in various cell types (17, 19, 20, 24). GGPP suppresses statin-induced cell death in various cell lines (17, 19, 20). Geranylgeraniol, a precursor of GGPP, can suppress statin-associated muscle symptoms in rats (25). These observations suggest that combined treatment with statins and fibrates induces cell death in myoblasts and myotubes by inhibiting GGPP biosynthesis.

GGPP is an important factor in the prenylation of small GTPases, such as Ras and Rho, and its prenylation is required for membrane anchoring of Ras and Rho (16, 26-30). The results of the present study showed that co-treatment with statins and bezafibrate did not suppress activation of p38MAPK, Akt, and ERK1/2, which are downstream of Ras in L6 myoblasts, but it significantly inhibited Rho activation. Rho activation regulates cell cycle progression through suppression of p27, p21, and p53 expression (21). Combined administration of statins and bezafibrate enhanced G1 and sub-G0/G1 populations by promoting p27 expression, but not p21 and p53 expression, or caspase-3 activity in L6 myoblasts. Rho activation promotes mDia, Rho kinase (ROCK), and citron kinase (31). mDia regulates actin polymerization, ROCK modulates reduced actin polymerization and increases actomyosin contractility, and citron kinase regulates cytokinesis (31). In addition, activation of ROCK decreases p27 expression and promotes cell cycle progression (32). Lovastatin suppresses cell proliferation by suppressing Rho

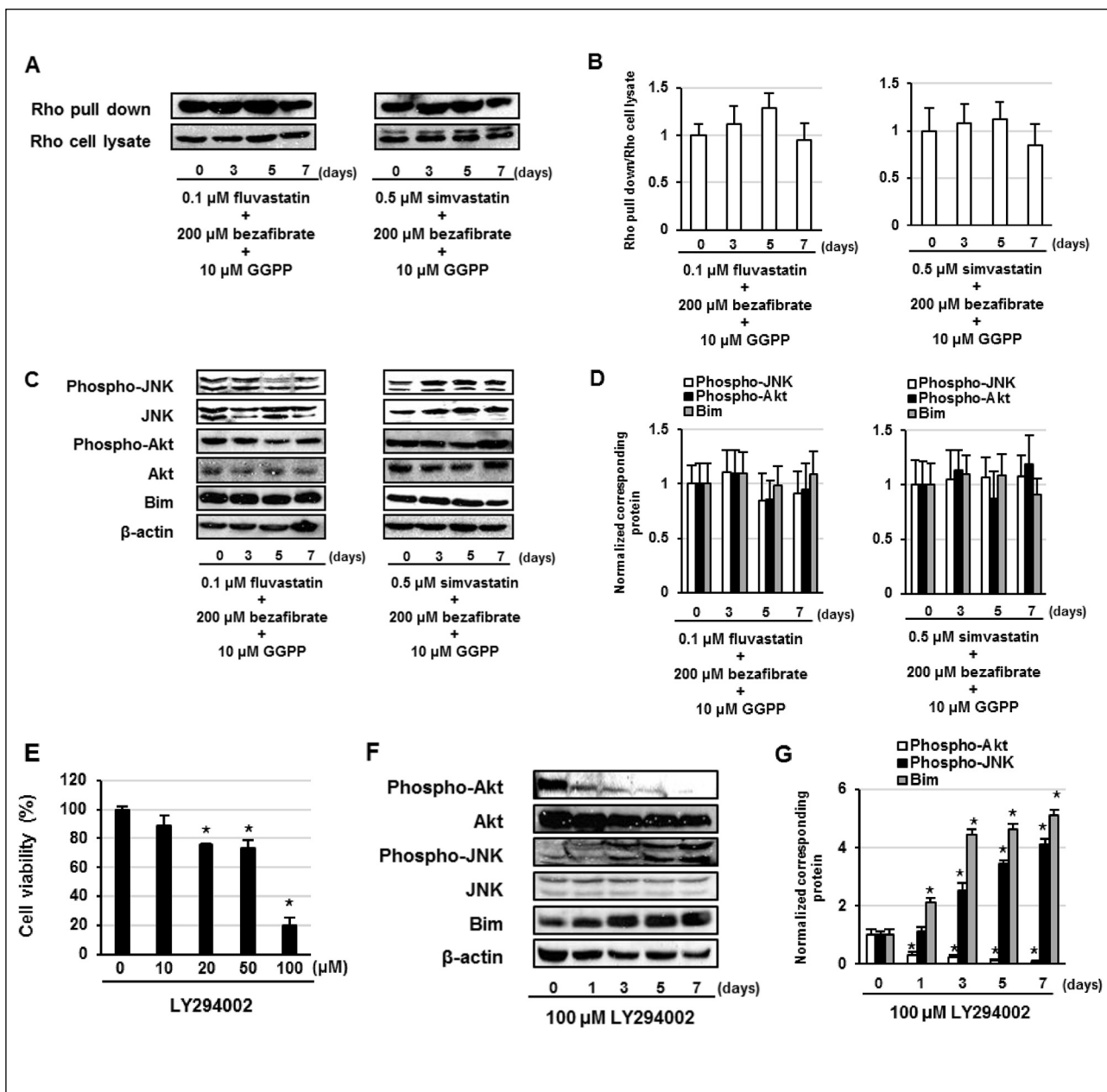
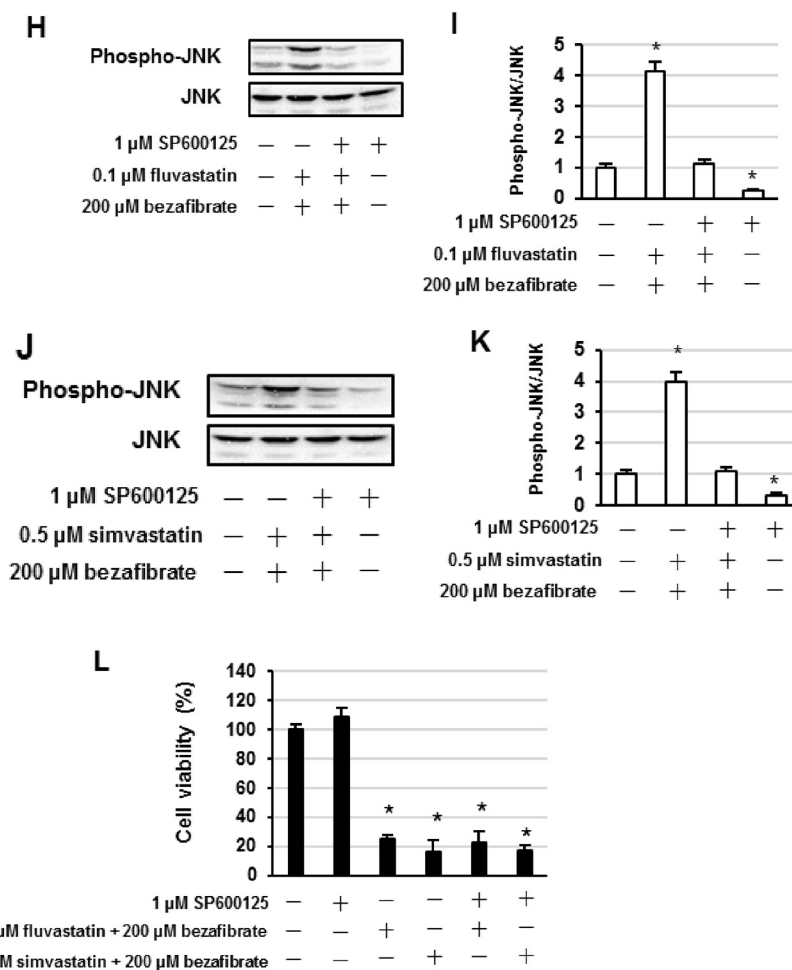


**Fig. 7.** Pretreatment with GGPP inhibits Rho and Akt inactivation in L6 myotube cells induced by co-treatment with statins and bezafibrate. L6 myotube cells were pretreated with 10  $\mu$ M GGPP for 4 h followed by treatment with fluvastatin or simvastatin in combination with bezafibrate for three, five, or seven days. (A): Western blots for the Rho-GTP form (Rho pull-down) and Rho cell lysate. (B): Amounts of Rho pull-down were measured and standardized to the amounts of the Rho cell lysate. Shown are the means  $\pm$  SD of three independent replicates.  $*P < 0.01$  vs. controls (ANOVA with Dunnett's test). (C): Cell lysates were subjected to Western blotting using phosphorylated phosphotyrosine (phospho-JNK), Akt (phospho-Akt), Bim, JNK, Akt, and  $\beta$ -actin antibodies. (D): Amounts of phospho-JNK, phospho-Akt, or Bim were measured and standardized to the amounts of the JNK, Akt, or  $\beta$ -actin. Shown are the means  $\pm$  SD of three independent replicates.  $*P < 0.01$  vs. controls (ANOVA with Dunnett's test). (E): Cell viability as observed by treatment with LY294002 in L6 myotube cells as determined with WST-8 assay. Cells were treated with LY294002 at different concentrations for seven days. Shown are the means  $\pm$  SD of five independent replicates.  $*P < 0.01$  vs. controls (ANOVA with Dunnett's test). (F): Cell lysates were subjected to Western blotting using phosphorylated Akt (phospho-Akt), phosphorylated JNK (phospho-JNK), Bim, Akt, JNK, and  $\beta$ -actin antibodies. (G): Amounts of phospho-Akt, phospho-JNK, or Bim were measured and standardized to the amounts of the Akt, JNK, or  $\beta$ -actin. Shown are the means  $\pm$  SD of three independent replicates.  $*P < 0.01$  vs. controls (ANOVA with Dunnett's test). (H-L): Effects of SP600125 on combination with statins and bezafibrate-induced L6 myotube cell death. Cells were treated with 1  $\mu$ M SP600125, 0.1  $\mu$ M fluvastatin, 0.5  $\mu$ M simvastatin, or 200  $\mu$ M bezafibrate alone or in combination for seven days. (H, J): Cell lysates were subjected to Western blotting using phosphorylated JNK (phospho-JNK) and JNK antibodies. (I, K): Amounts of phospho-JNK were measured and standardized to the amounts of JNK. Shown are the means  $\pm$  SD of three independent replicates.  $*P < 0.01$  vs. controls (ANOVA with Dunnett's test). (L) Cell viability after treatment with 1  $\mu$ M SP600125, 0.1  $\mu$ M fluvastatin, 0.5  $\mu$ M simvastatin, or 200  $\mu$ M bezafibrate alone, or in combination for seven days in L6 myotube cells, as determined using a WST-8 assay. Shown are the means  $\pm$  SD of five independent replicates.  $*P < 0.01$  vs. controls (ANOVA with Dunnett's test).



activation and increasing p27 expression in human anaplastic thyroid cancer cells (33). Moreover, simvastatin suppresses RhoA membrane translocation and enhances p27 expression in pulmonary artery smooth muscle cells (34). In addition, fenofibrate increases p27 expression by modulating the PPAR $\alpha$ /fork-head box O (FOXO) 1 pathway in human glioblastoma cells, thereby suppressing cell proliferation (35). Moreover, fenofibrate increased p27 expression by regulating the PPAR $\alpha$ /RB/DNA methyltransferase 1 and PPAR $\alpha$ /RB/ protein arginine methyltransferase 6 axes in colon carcinogenesis (36). Collectively, these findings suggest that combined treatment with statins and bezafibrate induces cell death in L6 myoblasts through suppression of Rho activation and induced upregulated p27 expression.

In contrast, we found that co-administration of statins and bezafibrate induced cell death in L6 myotubes through suppression of the Rho/Akt pathway and enhanced JNK activation and Bim expression. Moreover, PI3K inhibitor LY294002 induced cell death through inhibition of Akt activation and increased activation of JNK and Bim expression in L6 myotubes; however, JNK inhibitor SP600125 did not suppress the effects of combined treatment with statins and bezafibrate, thus inducing cell death. Simvastatin suppresses Akt activation, leading to inhibition of FOXO1 and FOXO3 phosphorylation in an *in vivo* model of statin-induced myopathy (37). Akt activation regulates FOXO1 and FOXO3 activation,

thereby suppressing the transcription of target genes such as Bim (38). Further, fenofibrate induces apoptosis by increasing FOXO3 and Bim expression in human glioblastoma cells (39), and FOXO1 promotes Bim transcription and induces apoptosis (40). These findings suggest that combined administration of statins and bezafibrate would induce L6 myotube cell death through inhibition of the Rho/Akt pathway and enhanced Bim expression.

Statins and PPAR $\alpha$  ligands induce cell death in myotubes but do not exhibit synergetic effects in cotreatments (41). This indicated that combination of atorvastatin and bezafibrate may induce apoptosis in L6 myotubes (42). In addition, co-treatment with cerivastatin, pitavastatin, and gemfibrozil markedly induces cell death in L6 myoblasts (43). Taken together, our results suggest that combination of statins and bezafibrate markedly induced cell death in myoblasts and myotubes.

Recently, hypoxia does not affect myoblast proliferation and survival, but promotes HIF-1 $\alpha$  expression and angiogenesis, suggesting that it may be useful for tissue regeneration after myocardial infarction (44). It has also indicated that 1-trifluoromethoxyphenyl-3-(1-propionylpiperidine-4-yl) urea, a soluble epoxide hydrolase inhibitor, occurred *via* regeneration by promoting the angiogenesis, endothelial cell proliferation and neovascularization (45). In addition, it has indicated that treatment with resveratrol at non-toxic doses suppressed LDL cholesterol without lowering HDL and total cholesterol in type 2

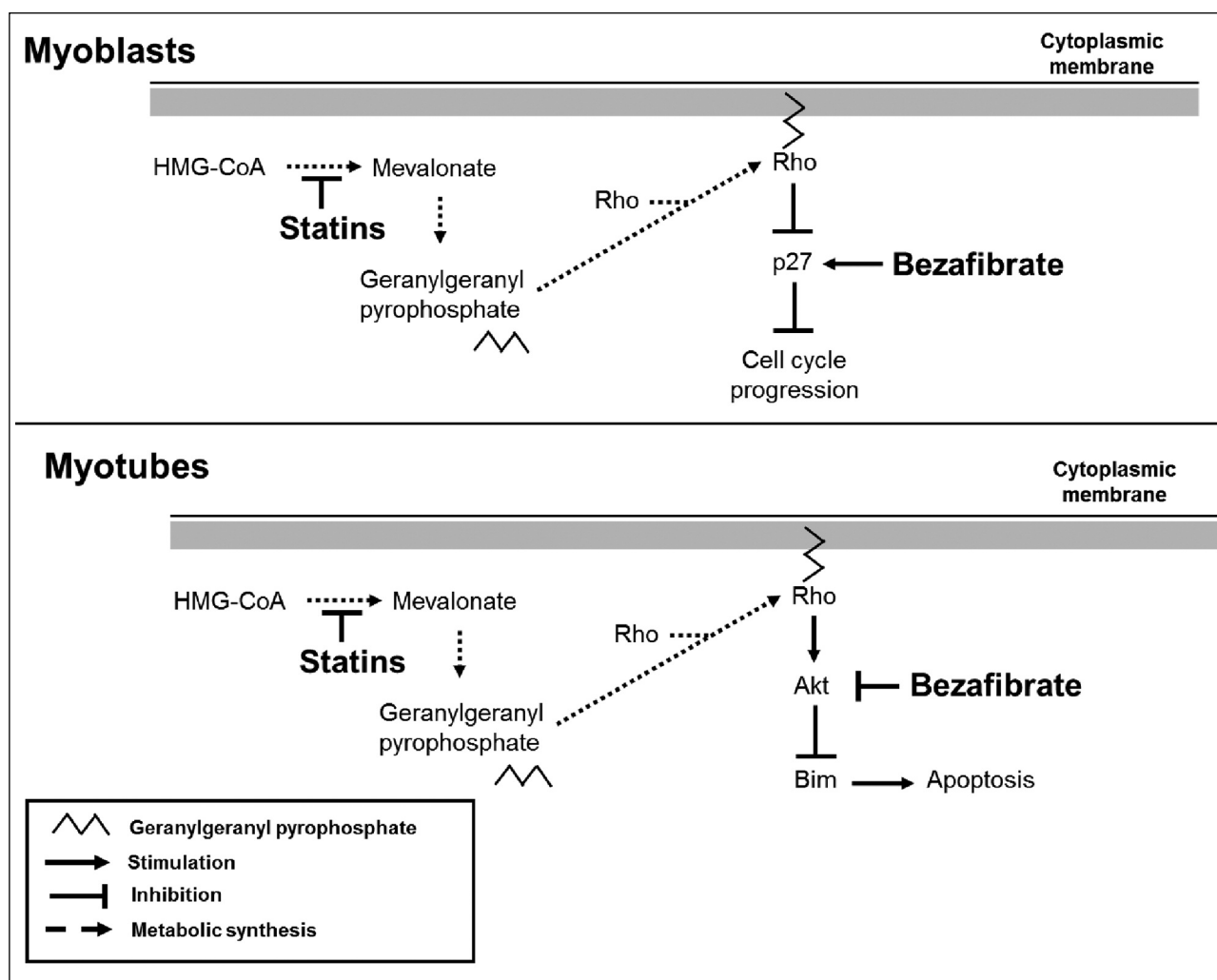


Fig. 8. Cytotoxic effects of combined treatment with statins and bezafibrate on myoblasts and myotubes.

diabetic rats (46). These findings suggest that tissue regeneration by hypoxia and treatment with resveratrol may be useful during muscle injury with statin and fibrate administration.

The results of this study showed that combined treatment with statins and fibrates induced cell death in L6 myoblasts and myotube cells through inhibition of GGPP biosynthesis and Rho pathway activation. Drug combination-induced L6 myoblast cell death was associated with enhanced p27 expression, leading to promotion of G1 arrest (Fig. 8). Moreover, drug combination-induced L6 myotube cell death was also associated with suppression of Akt activation and increased expression of Bim (Fig. 8). These results indicated that supplementation with GGPP may be therapeutically beneficial for preventing myotoxicity induced by co-treatment with statins and fibrates.

**Authors' contribution:** Conceptualization: S. Nishida, M. Tsubaki; formal analysis and writing - original draft: T. Takeda, T. Mastuda, A. Kimura, M. Yanae, A. Maeda, T. Hoshida, and formal analysis: K. Tanabe.

**Acknowledgements:** This work was supported in part by a Grant-in-Aid for Scientific Research (C) (Grant numbers 20K07145 and 20K07168) from the Japan Society for the Promotion of Science (JSPS).

Conflicts of interests: None declared.

## REFERENCES

1. Oshima Y. Characteristics of drug-associated rhabdomyolysis: analysis of 8,610 cases reported to the U.S. Food and Drug Administration. *Intern Med* 2011; 50: 845-853.
2. Bosch X, Poch E, Grau JM. Rhabdomyolysis and acute kidney injury. *N Engl J Med* 2009; 361: 62-72.
3. Enger C, Gately R, Ming EE, Niemcryk SJ, Williams L, McAfee AT. Pharmacoeconomics safety study of fibrate and statin concomitant therapy. *Am J Cardiol* 2010; 106: 1594-1601.
4. Bouitbir J, Sanvee GM, Panajatovic MV, Singh F, Krahenbuhl S. Mechanisms of statin-associated skeletal muscle-associated symptoms. *Pharmacol Res* 2020; 154: 104201. doi: 10.1016/j.phrs.2019.03.010
5. Apostolopoulou M, Corsini A, Roden M. The role of mitochondria in statin-induced myopathy. *Eur J Clin Invest* 2015; 45: 745-754.

6. Ahmadi Y, Ghorbanihaghjo A, Argani H. The balance between induction and inhibition of mevalonate pathway regulates cancer suppression by statins: A review of molecular mechanisms. *Chem Biol Interact* 2017; 273: 273-285.
7. De Luca A, Pierno S, Camerino DC. Electrical properties of diaphragm and EDL muscles during the life of dystrophic mice. *Am J Physiol* 1997; 272: C333-C340.
8. Hong F, Xu P, Zhai Y. The opportunities and challenges of peroxisome proliferator-activated receptors ligands in clinical drug discovery and development. *Int J Mol Sci* 2018; 19: 2189. doi: 10.3390/ijms19082189
9. Zhao Y, Okuyama M, Hashimoto H, Tagawa Y, Jomori T, Yang B. Bezafibrate induces myotoxicity in human rhabdomyosarcoma cells via peroxisome proliferator-activated receptor alpha signaling. *Toxicol In Vitro* 2010; 24: 154-159.
10. Roy A, Jana M, Kundu M, et al. HMG-CoA reductase inhibitors bind to ppara to upregulate neurotrophin expression in the brain and improve memory in mice. *Cell Metab* 2015; 22: 253-265.
11. Seo M, Inoue I, Ikeda M, et al. Statins activate human PPARalpha promoter and increase PPARalpha mRNA expression and activation in HepG2 cells. *PPAR Res* 2008; 2008: 316306. doi: 10.1155/2008/316306
12. Stahlberg D, Angelin B, Einarsson K. Effects of treatment with clofibrate, bezafibrate, and ciprofibrate on the metabolism of cholesterol in rat liver microsomes. *J Lipid Res* 1989; 30: 953-958.
13. Maiguma T, Fujisaki K, Itoh Y, et al. Cell-specific toxicity of fibrates in human embryonal rhabdomyosarcoma cells. *Naunyn Schmiedeberg's Arch Pharmacol* 2003; 367: 289-296.
14. Owczarek J, Jasińska M, Orszulak-Michalak D. Drug-induced myopathies. An overview of the possible mechanisms. *Pharmacol Rep* 2005; 57: 23-34.
15. Morii Y, Tsubaki M, Takeda T, et al. Perifosine enhances the potential antitumor effect of 5-fluorouracil and oxaliplatin in colon cancer cells harboring the PIK3CA mutation. *Eur J Pharmacol* 2021; 898: 173957. doi: 10.1016/j.ejphar.2021.173957
16. Tanimori Y, Tsubaki M, Yamazoe Y, et al. Nitrogen-containing bisphosphonate, YM529/ONO-5920, inhibits tumor metastasis in mouse melanoma through suppression of the Rho/ROCK pathway. *Clin Exp Metastasis* 2010; 27: 529-538.
17. Fujiwara D, Tsubaki M, Takeda T, et al. Statins induce apoptosis through inhibition of Ras signaling pathways and enhancement of Bim and p27 expression in human hematopoietic tumor cells. *Tumour Biol* 2017; 39: 1010428317734947. doi: 10.1177/1010428317734947
18. Chou TC, Talalay P. Quantitative analysis of dose-effect relationships: the combined effects of multiple drugs or enzyme inhibitors. *Adv Enzyme Regul* 1984; 22: 27-55.
19. Tsubaki M, Fujiwara D, Takeda T, et al. The sensitivity of head and neck carcinoma cells to statins is related to the expression of their Ras expression status, and statin-induced apoptosis is mediated via suppression of the Ras/ERK and Ras/mTOR pathways. *Clin Exp Pharmacol Physiol* 2017; 44: 222-234.
20. Yanae M, Tsubaki M, Satou T, et al. Statin-induced apoptosis via the suppression of ERK1/2 and Akt activation by inhibition of the geranylgeranyl-pyrophosphate biosynthesis in glioblastoma. *J Exp Clin Cancer Res* 2011; 30: 74. doi: 10.1186/1756-9966-30-74
21. Tsubaki M, Takeda T, Kino T, et al. Statins improve survival by inhibiting spontaneous metastasis and tumor growth in a mouse melanoma model. *Am J Cancer Res* 2015; 5: 3186-3197.
22. Tsubaki M, Takeda T, Tomonari Y, et al. The MIP-1α autocrine loop contributes to decreased sensitivity to anticancer drugs. *J Cell Physiol* 2018; 233: 4258-4271.
23. Tan JT, Barry AR. Coenzyme Q10 supplementation in the management of statin-associated myalgia. *Am J Health Syst Pharm* 2017; 74: 786-793.
24. Johnson TE, Zhang X, Bleicher KB, et al. Statins induce apoptosis in rat and human myotube cultures by inhibiting protein geranylgeranylation but not ubiquinone. *Toxicol Appl Pharmacol* 2004; 200: 237-250.
25. Irwin JC, Fenning AS, Vella RK. Geranylgeraniol prevents statin-induced skeletal muscle fatigue without causing adverse effects in cardiac or vascular smooth muscle performance. *Transl Res* 2020; 215: 17-30.
26. Kidera Y, Tsubaki M, Yamazoe Y, et al. Reduction of lung metastasis, cell invasion, and adhesion in mouse melanoma by statin-induced blockade of the Rho/Rho-associated coiled-coil-containing protein kinase pathway. *J Exp Clin Cancer Res* 2010; 29: 127. doi: 10.1186/1756-9966-29-127
27. Tsubaki M, Mashimo K, Takeda T, et al. Statins inhibited the MIP-1α expression via inhibition of Ras/ERK and Ras/Akt pathways in myeloma cells. *Biomed Pharmacother* 2016; 78: 23-29.
28. Tsubaki M, Takeda T, Sakamoto K, et al. Bisphosphonates and statins inhibit expression and secretion of MIP-1α via suppression of Ras/MEK/ERK/AML-1A and Ras/PI3K/Akt/AML-1A pathways. *Am J Cancer Res* 2014; 5: 168-179.
29. Tsubaki M, Itoh T, Satou T, et al. Nitrogen-containing bisphosphonates induce apoptosis of hematopoietic tumor cells via inhibition of Ras signaling pathways and Bim-mediated activation of the intrinsic apoptotic pathway. *Biochem Pharmacol* 2013; 85: 163-172.
30. Tsubaki M, Satou T, Itoh T, et al. Reduction of metastasis, cell invasion, and adhesion in mouse osteosarcoma by YM529/ONO-5920-induced blockade of the Ras/MEK/ERK and Ras/PI3K/Akt pathway. *Toxicol Appl Pharmacol* 2012; 259: 402-410.
31. Mosaddeghzadeh N, Ahmadian MR. The RHO Family GTPases: Mechanisms of regulation and signaling. *Cells* 2021; 10: 1831. doi: 10.3390/cells10071831
32. Croft DR, Olson MF. The Rho GTPase effector ROCK regulates cyclin A, cyclin D1, and p27Kip1 levels by distinct mechanisms. *Mol Cell Biol* 2006; 26: 4612-4627.
33. Zhong WB, Hsu SP, Ho PY, Liang YC, Chang TC, Lee WS. Lovastatin inhibits proliferation of anaplastic thyroid cancer cells through up-regulation of p27 by interfering with the Rho/ROCK-mediated pathway. *Biochem Pharmacol* 2011; 82: 1663-1672.
34. Ikeda T, Nakamura K, Akagi S, et al. Inhibitory effects of simvastatin on platelet-derived growth factor signaling in pulmonary artery smooth muscle cells from patients with idiopathic pulmonary arterial hypertension. *J Cardiovasc Pharmacol* 2010; 55: 39-48.
35. Han DF, Zhang JX, Wei WJ, et al. Fenofibrate induces G0/G1 phase arrest by modulating the PPARα/FoxO1/p27 kip pathway in human glioblastoma cells. *Tumour Biol* 2015; 36: 3823-3829.
36. Luo Y, Xie C, Brocker CN, et al. Intestinal PPARα protects against colon carcinogenesis via regulation of methyltransferases DNMT1 and PRMT6. *Gastroenterology* 2019; 157: 744-759.e4.
37. Mallinson JE, Constantin-Teodosiu D, Sidaway J, Westwood FR, Greenhaff PL. Blunted Akt/FOXO signalling and activation of genes controlling atrophy and fuel use in statin myopathy. *J Physiol* 2009; 587: 219-230.
38. Lv Y, Song S, Zhang K, Gao H, Ma R. CHIP regulates AKT/FoxO/Bim signaling in MCF7 and MCF10A cells. *PLoS One* 2013; 8: e83312. doi: 10.1371/journal.pone.0083312
39. Wilk A, Urbanska K, Grabacka M, et al. Fenofibrate-induced nuclear translocation of FoxO3A triggers Bim-

- mediated apoptosis in glioblastoma cells in vitro. *Cell Cycle* 2012; 11: 2660-2671.
40. Xing YQ, Li A, Yang Y, Li XX, Zhang LN, Guo HC. The regulation of FOXO1 and its role in disease progression. *Life Sci* 2018; 193: 124-131.
  41. Johnson TE, Zhang X, Shi S, Umbenhauer DR. Statins and PPARalpha agonists induce myotoxicity in differentiated rat skeletal muscle cultures but do not exhibit synergy with co-treatment. *Toxicol Appl Pharmacol* 2005; 208: 210-221.
  42. Matzno S, Tazuya-Murayama K, Tanaka H, *et al.* Evaluation of the synergistic adverse effects of concomitant therapy with statins and fibrates on rhabdomyolysis. *J Pharm Pharmacol* 2003; 55: 795-802.
  43. Morikawa S, Murakami T, Yamazaki H, *et al.* Analysis of the global RNA expression profiles of skeletal muscle cells treated with statins. *J Atheroscler Thromb* 2005; 12: 121-131.
  44. Zimna A, Wiernicki B, Kolanowski T, *et al.* Influence of hypoxia prevailing in post-infarction heart on proangiogenic gene expression and biological features of human myoblast cells applied as a pro-regenerative therapeutic tool. *J Physiol Pharmacol* 2018; 69: 859-874.
  45. Shah SA, Mehmood MH, Khan M, Bukhari IA, Alorainey BI, Vohra F. Inhibition of soluble epoxide hydrolase offers protection against fructose-induced diabetes and related metabolic complications in rats. *J Physiol Pharmacol* 2020; 71: 615-624.
  46. Szkudelska K, Okulicz M, Szkudelski T. Resveratrol reduces excessive cholesterol accumulation in Goto-Kakizaki rat, a model with congenital type 2 diabetes. *J Physiol Pharmacol* 2020; 71: 581-587.

Received: January 28, 2022

Accepted: February 28, 2022

Author's address: Dr. Shozo Nishida, Division of Pharmacotherapy, Kinki University School of Pharmacy, Kowakae, Higashi-Osaka 577-8502, Japan.

E-mail address: nishida@phar.kindai.ac.jp